

Organic Photothermal Cocrysal with High Stability for Efficient Solar-driven Water Evaporation

Mengjia Jiang^{†a}, Yi Su^{†a}, Shuyu Li^b, Siyao Fu^a, Lingsong Wang^a, Darya khan^a, Yajing Sun^{*a}, Lingjie Sun^{*a,c}, Xiaotao Zhang^{*b}, Wenping Hu^{a,c}

a.Tianjin Key Laboratory of Molecular Optoelectronic Sciences, Department of Chemistry, School of Science, Tianjin University, Tianjin 300072, China

b.Institute of Molecular Aggregation Science of Tianjin University, Tianjin 300072, China

c.Joint School of National University of Singapore and Tianjin University, International Campus of Tianjin University, Fuzhou 350207, China

[*] Corresponding Authors: zhangxt@tju.edu.cn; sunlingjie@tju.edu.cn; syj19@tju.edu.cn

1. Supplemental Figures and Table

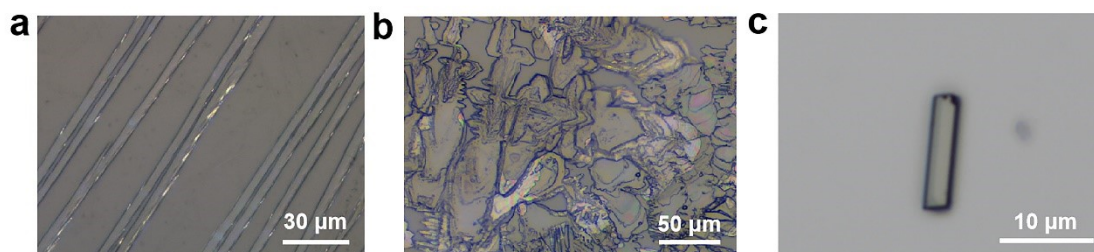


Fig S1. Optical microscope images of (a) TMBZ crystal, (b) TCNB crystal, (c) TMBZ-TCNB cocrysal obtained from drop casting on the quartz substrate.

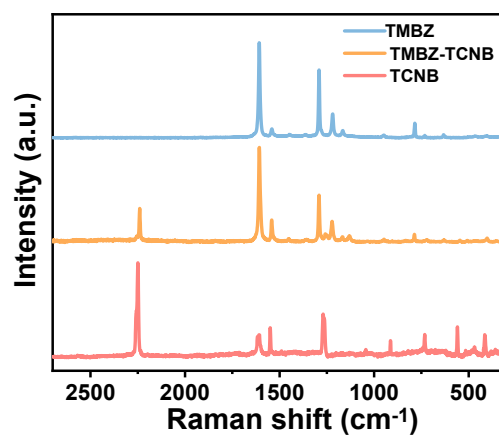


Fig S2. Raman spectrum of TMBZ, TCNB, and TMBZ-TCNB cocrysal.

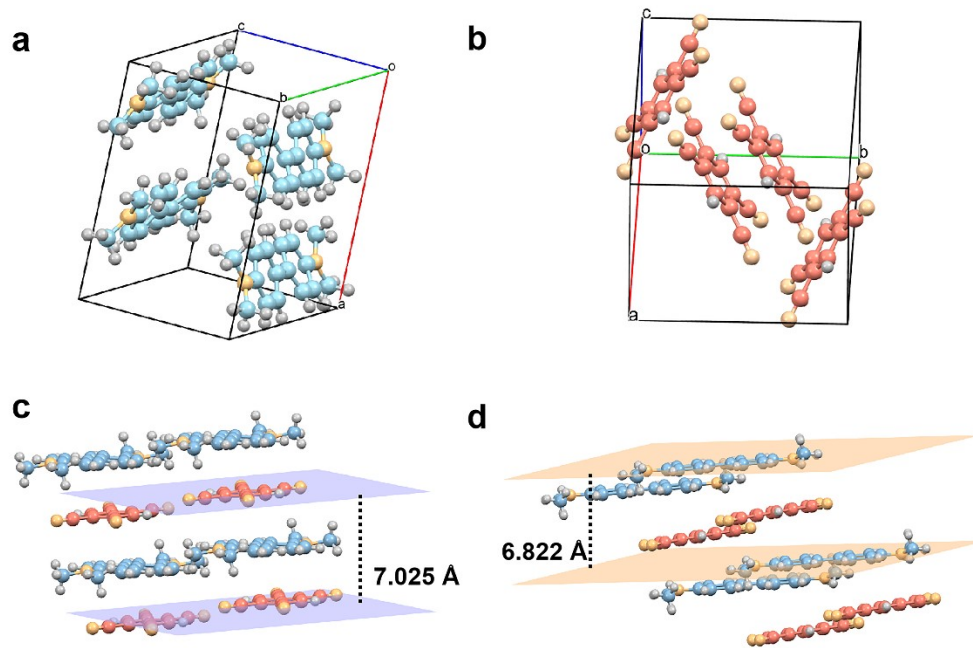


Fig S3. Packing structure of (a) TMBZ and (b) TCNB. The distance between the (c) two adjacent donors and (d) two adjacent acceptors.

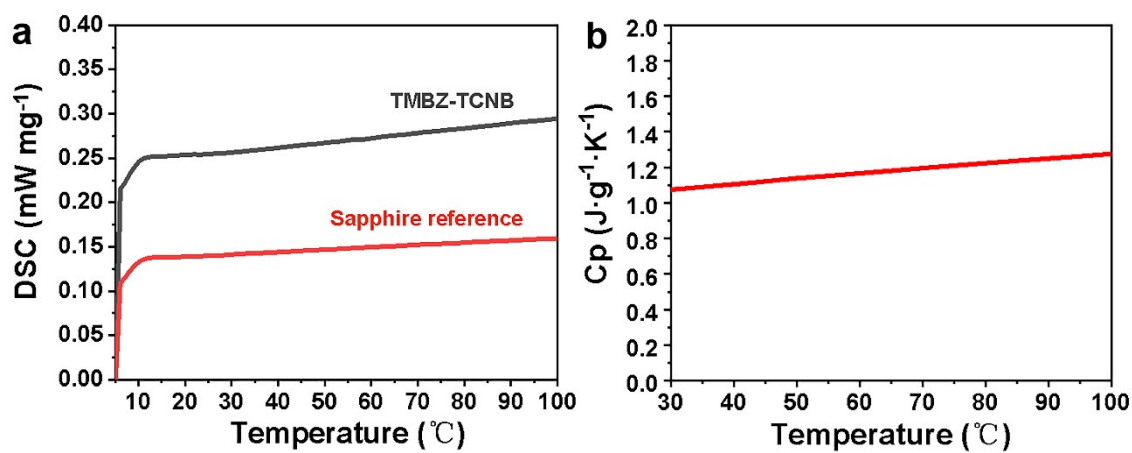


Fig S4. (a) DSC curves of the cocrystal and sapphire reference. (b) Specific heat capacity results of the TMBZ-TCNB cocrystal.

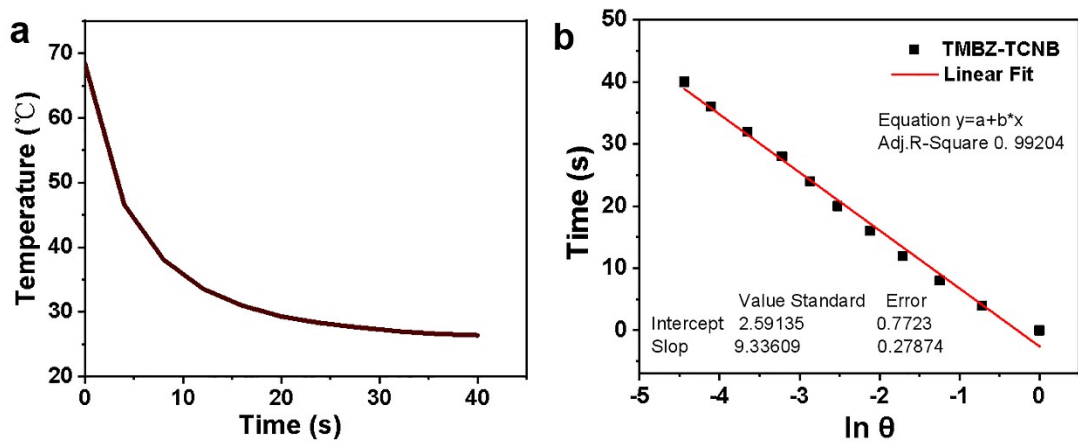


Fig S5. (a) The cooling curve of TMBZ-TCNB cocrystal under the irradiation of 808 nm laser and (b) corresponding time- $\ln\theta$ linear curve.

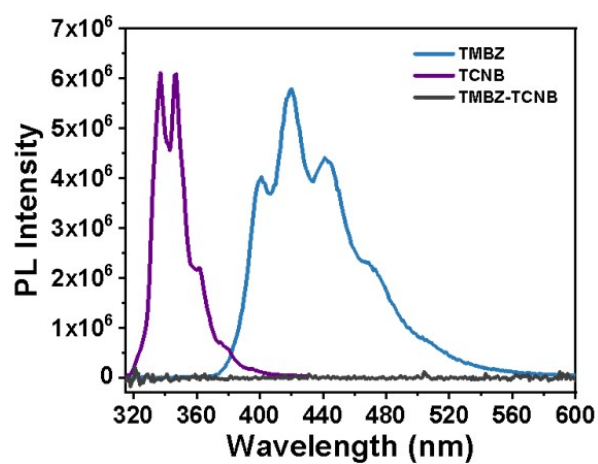


Fig S6. Fluorescence spectra of TMBZ, TCNB, and TMBZ-TCNB.

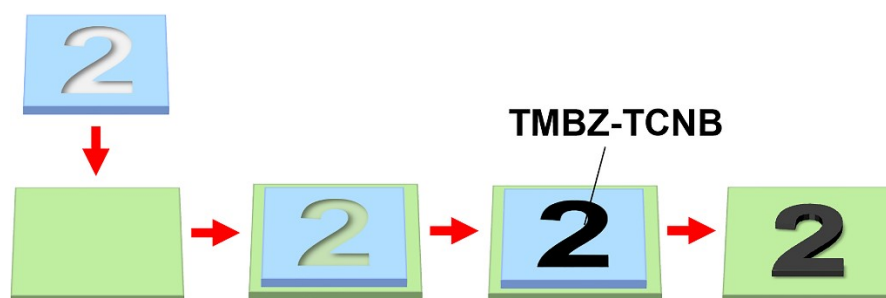


Fig S7. The patterning process of letter "2023".

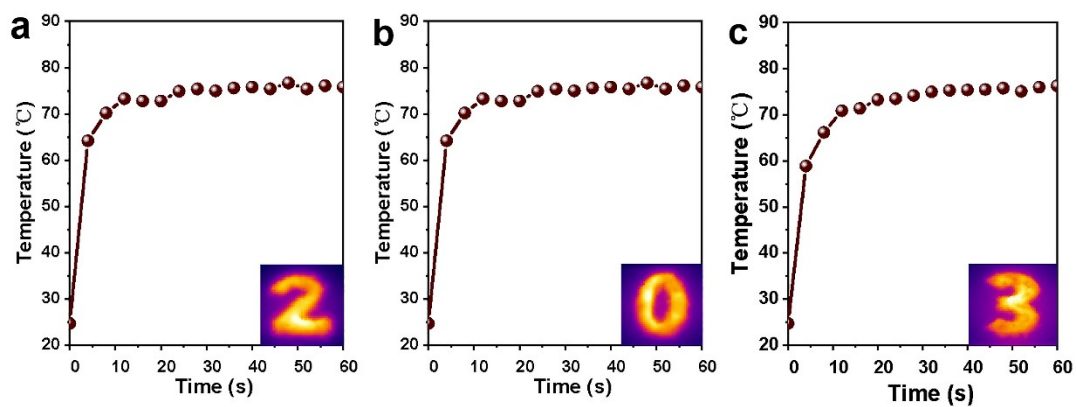


Fig S8. The temperature change curves of photothermal imaging for (a) “2”, (b) “0”, and (c) “3”.

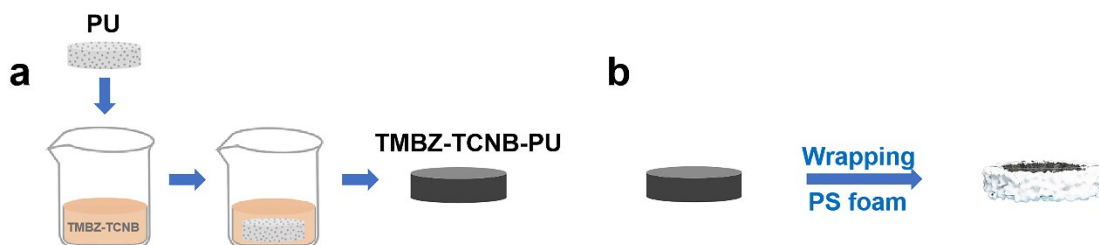


Fig S9. The schematic of process for PU sponge loading TMBZ-TCNB by impregnation method.

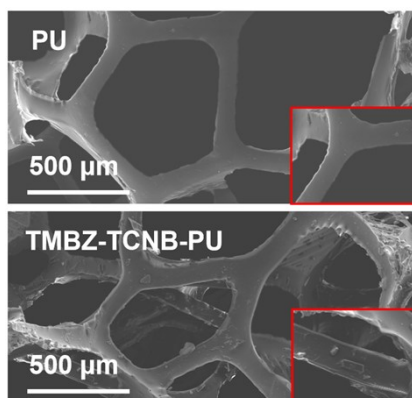


Fig S10. SEM images of PU (top) and TMBZ-TCNB-PU (bottom).

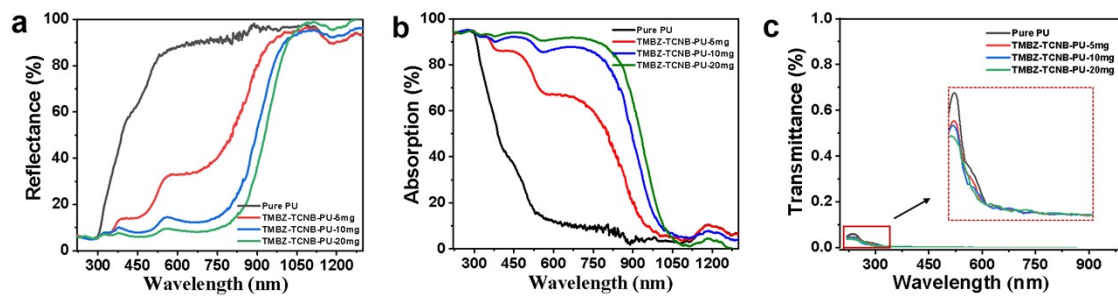


Fig S11. (a) The absorption, (b) reflectance and (c) transmittance spectra of PU with different loading amounts of TMBZ-TCNB.

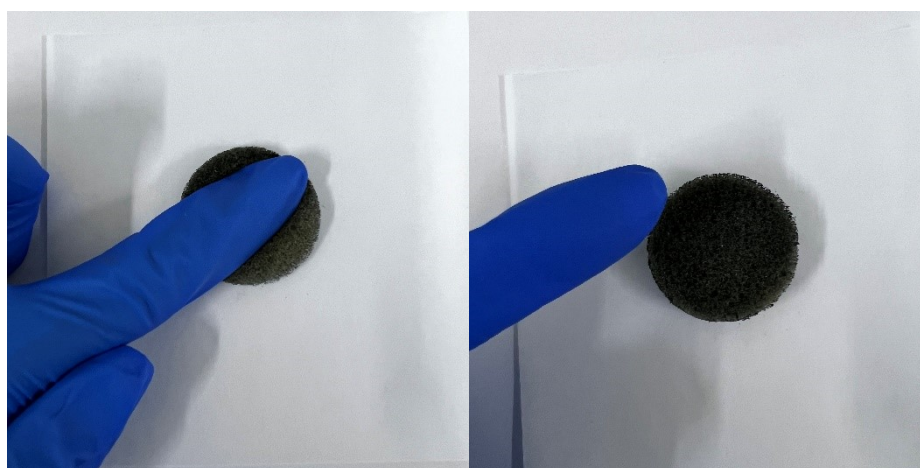


Fig S12. Digital photographs showing that the TMBZ-TCNB cocystal was firmly attached to the surface of PU

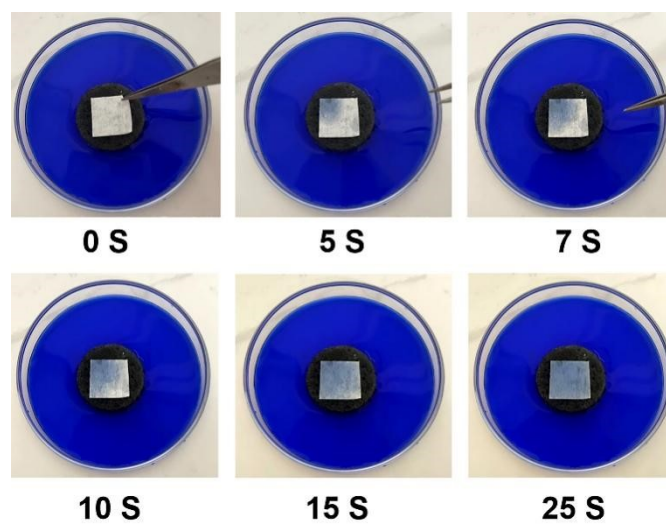


Fig S13. Water transport experiment of PU-TMBZ-TCNB.

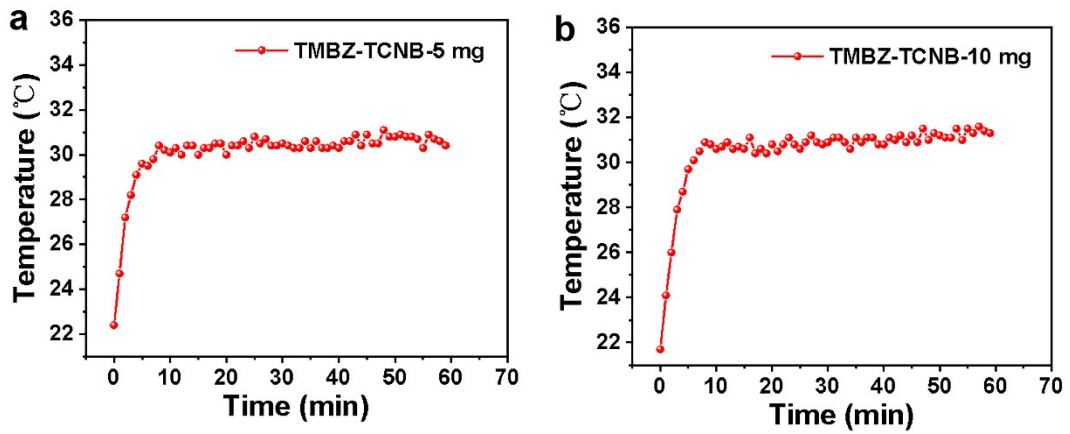


Fig S14. The temperature change curves of (a) TMBZ-TCNB-PU-5 mg and (b) TMBZ-TCNB-PU-10 mg under the solar irradiation of $1 \text{ kW}\cdot\text{m}^{-2}$.

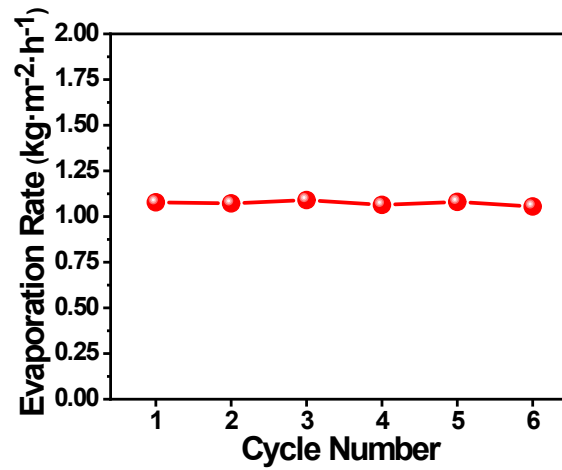


Fig S15. Cycling test of TMBZ-TCNB-PU under solar irradiation of $1 \text{ kW}\cdot\text{m}^{-2}$.

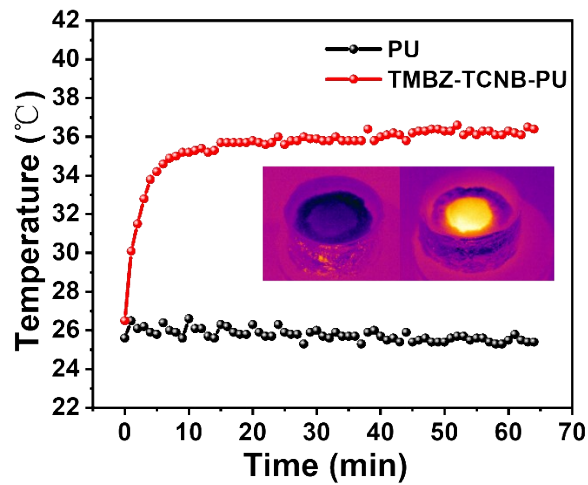


Fig S16. The temperature change curves of PU the TMBZ-TCNB-PU of 20 mg in the simulated seawater under the solar irradiation of $1 \text{ kW}\cdot\text{m}^{-2}$.

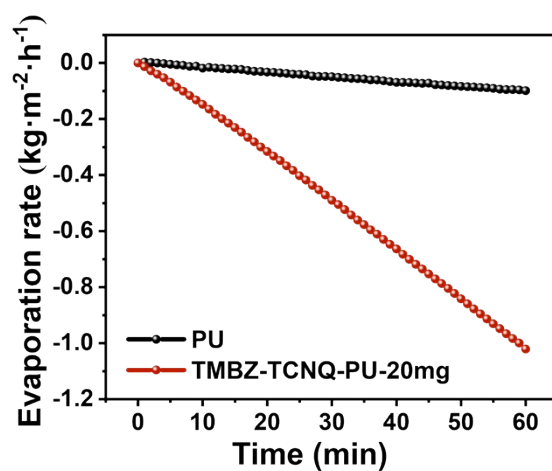


Fig S17. Water evaporation curves of PU and TMBZ-TCNB-PU with 20mg of TMBZ-TCNB loading in the simulated seawater under the solar irradiation of $1 \text{ kW}\cdot\text{m}^{-2}$.

Table S1. Single crystal structure of TMBZ-TCNB cocrystal

Parameter	Value/Comment
Empirical formula	$\text{C}_{26}\text{H}_{22}\text{N}_6$
CCDC number	2271812
Formula weight	418.5
Wavelength	1.542
Crystal system	triclinic
Space group	P-1
a (Å)	7.6949(7)
b (Å)	8.0542(7)
c (Å)	9.7834(8)
α (deg)	101.397(7)
β (deg)	104.755(7)
γ (deg)	101.687(7)
Volume (Å ³)	553.95(9)
Z	2
ρ_{calc} (g·cm ⁻³)	1.254
μ (mm ⁻¹)	0.612
F(000)	220.0
Independent reflections	$R_{\text{int}}=0.0149$, $R_{\text{sigma}}=0.0194$
Goodness-of-fit on F^2	1.042
Final R indices [$I > 2\sigma(I)$]	$R_1=0.0434$, $wR_2=0.1236$
Final R indices [all data]	$R_1=0.0495$, $wR_2=0.1308$

2. Calculation of the photothermal conversion efficiency

The photothermal conversion efficiency of TMBZ-TCNB is calculated according to the previous method¹. The formulas are as follows:

Based on the total energy balance of the whole system:

$$\sum_i m_i C_{p,i} \frac{dT}{dt} = Q_s - Q_{loss}$$

Where m_i (75 mg) and $C_{p,i}$ ($1.18 \text{ J} \cdot (\text{g} \cdot ^\circ\text{C})^{-1}$) represent the mass and specific heat capacity of the photothermal system, respectively. The Q_s is the input energy by 808 nm laser irradiation, and Q_{loss} is the energy loss to surrounding environment. The system reaches thermal equilibrium when the temperature reaches to the maximum.

$$Q_s = Q_{loss} = hS\Delta T_{max}$$

Where h represents the heat transfer coefficient, S represents the surface area of the system, and ΔT_{max} ($42.5 \text{ }^\circ\text{C}$) represents the maximum temperature change value of the system.

The photothermal conversion efficiency η can be calculated by the following equation:

$$\eta = \frac{hS\Delta T_{max}}{I(1 - 10^{-A_{808}})}$$

Where I represents the laser power ($0.6 \text{ W} \cdot \text{cm}^{-2}$). And the A_{808} (0.82) is the absorbance of the system at 808 nm.

In order to obtain the hS , a dimensionless driving force temperature, θ is introduced as following:

$$\theta = \frac{T - T_{surr}}{T_{max} - T_{surr}}$$

Where T is the real-time temperature of the system, T_{max} ($68.4 \text{ }^\circ\text{C}$) is the maximum temperature of the system, T_{surr} ($25.9 \text{ }^\circ\text{C}$) is the initial temperature of the system.

The time constant τ_s of sample system:

$$\tau_s = \frac{\sum_i m_i C_{p,i}}{hS}$$

Then:

$$\frac{d\theta}{dt} = \frac{1}{\tau_s} \frac{Q_s}{hS\Delta T_{max}} - \frac{\theta}{\tau_s}$$

After the laser is off, $Q_s = 0$, thus $\frac{d\theta}{dt} = -\frac{\theta}{\tau_s}$, and $t = -\tau_s \ln \theta$

so that the hS can be calculated through the slope of cooling time t vs $\ln \theta$. As result, τ_s is 9.34 s and the photothermal conversion efficiency is 59.46 %.

3. Calculation of the efficiency for solar to vapor generation

The formula for calculating conversion efficiency of solar for water evaporation is as follows^{2, 3}:

$$\eta = \frac{mh_{LV}}{C_{opt}P_o}$$

Where m represents the evaporation rate under simulated solar irradiation, C_{opt} (1) represents the optical concentration, P_o (1 km·cm⁻²) represents the solar irradiation density.

The m is calculated by the formula:

$$m = m_{light} - m_{dark}$$

m_{light} represents the water evaporation rate under simulated solar irradiation (1.078 kg·m⁻²·h⁻¹),

m_{dark} represents the water evaporation rate under dark condition (0.114 kg·m⁻²·h⁻¹).

h_{LV} is the phase change enthalpy of liquid water vapor of the system. The calculation formula is:

$$h_{LV} = Q + \Delta h_{vap}$$

Where Q represents the energy provided to heat the system from the initial temperature to a final temperature, and the calculation formula is:

$$Q = C_{liquid} \times (T - T_0)$$

C_{liquid} is the specific heat capacity of liquid water (4.18 kg⁻¹·K⁻¹), T_0 and T are the initial temperature (25 °C) and final temperature (32.3 °C) of the system.

Where Δh_{vap} represents the latent heat of vaporization of water, and the calculation formula is:

$$\Delta h_{vap} = Q_1 + \Delta h_{100} + Q_2$$

Q_1 is the energy released when temperature of liquid water rises from T to 100 °C, Δh_{100} (2260 kJ·kg⁻¹) is latent heat of vaporization of water at 100 °C, Q_2 is the energy released when temperature of water vapor drops from 100 °C to T . Q_1 and Q_2 can be calculated by:

$$Q_1 = C_{liquid} \times (100 - T)$$

$$Q_2 = C_{vapor} \times (T - 100)$$

C_{vapor} is the specific heat capacity of water vapor (1.865 kg⁻¹·k⁻¹).

So,

$$Q = C_{liquid} \times (T - T_0) = 4.18 \times (32.3 - 25) = 30.514 \text{ kJ} \cdot \text{kg}^{-1}$$

$$\Delta h_{vap} = Q_1 + \Delta h_{100} + Q_2 = 4.18 \times (100 - 32.3) + 2260 + 1.865 \times (32.3 - 100) = 2416.73 \text{ kJ} \cdot \text{kg}^{-1}$$

$$h_{LV} = Q + \Delta h_{vap} = 30.514 + 2416.73 = 2447.244 \text{ kJ} \cdot \text{kg}^{-1}$$

$$m = m_{light} - m_{dark} = 1.078 - 0.144 = 0.934 \text{ kg} \cdot \text{m}^{-2} \cdot \text{h}^{-1}$$

$$\eta = \frac{mh_{LV}}{C_{opt}P_o} = 63.49 \%$$

4. Calculation of the seawater evaporation efficiency

The formula for calculating conversion efficiency of solar for water evaporation is as follows^{2,3}:

$$\eta = \frac{m h_{LV}}{C_{opt} P_o}$$

Where m represents the evaporation rate under simulated solar irradiation, C_{opt} (1) represents the optical concentration, P_o (1 km·cm⁻²) represents the solar irradiation density.

The m is calculated by the formula:

$$m = m_{light} - m_{dark}$$

m_{light} represents the simulated seawater evaporation rate under simulated solar irradiation (1.021 kg·m⁻²·h⁻¹),

m_{dark} represents the simulated seawater evaporation rate under dark condition (0.099 kg·m⁻²·h⁻¹).

h_{LV} is the phase change enthalpy of liquid simulated seawater vapor of the system. The calculation formula is:

$$h_{LV} = Q + \Delta h_{vap}$$

Where Q represents the energy provided to heat the system from the initial temperature to a final temperature, and the calculation formula is:

$$Q = C_{liquid} \times (T - T_0)$$

C_{liquid} is the specific heat capacity of liquid simulated seawater (4.18 kg⁻¹·K⁻¹), T_0 and T are the initial temperature (26.5 °C) and final temperature (36.6 °C) of the system.

Where Δh_{vap} represents the latent heat of vaporization of simulated seawater, and the calculation formula is:

$$\Delta h_{vap} = Q_1 + \Delta h_{100} + Q_2$$

Q_1 is the energy released when temperature of liquid simulated seawater rises from T to 100 °C, Δh_{100} (2260 kJ·kg⁻¹) is latent heat of vaporization of simulated seawater at 100 °C, Q_2 is the energy released when temperature of simulated seawater vapor drops from 100 °C to T . Q_1 and Q_2 can be calculated by:

$$Q_1 = C_{liquid} \times (100 - T)$$

$$Q_2 = C_{vapor} \times (T - 100)$$

C_{vapor} is the specific heat capacity of simulated seawater vapor (1.865 kg⁻¹·K⁻¹).

So,

$$Q = C_{liquid} \times (T - T_0) = 4.18 \times (36.6 - 26.5) = 42.218 \text{ kJ} \cdot \text{kg}^{-1}$$

$$\Delta h_{vap} = Q_1 + \Delta h_{100} + Q_2 = 4.18 \times (100 - 36.6) + 2260 + 1.865 \times (36.6 - 100) = 2406.771 \text{ kJ} \cdot \text{kg}^{-1}$$

$$h_{LV} = Q + \Delta h_{vap} = 42.218 + 2406.771 = 2448.989 \text{ kJ} \cdot \text{kg}^{-1}$$

$$m = m_{light} - m_{dark} = 1.021 - 0.099 = 0.9222 \text{ kg} \cdot \text{m}^{-2} \cdot \text{h}^{-1}$$

$$\eta = \frac{m h_{LV}}{C_{opt} P_o} = 62.73 \%$$

Reference

1. Y. Wang, W. Zhu, W. Du, X. Liu, X. Zhang, H. Dong and W. Hu, *Angew. Chem. Int. Ed.*, 2018, **57**, 3963-3967.

2. J. Liu, Y. Cui, Y. Pan, Z. Chen, T. Jia, C. Li and Y. Wang, *Angew. Chem. Int. Ed.*, 2022, **61**, e202117087.
3. M. Gao, L. Zhu, C. K. Peh and G. W. Ho, *Energy Environ. Sci.*, 2019, **12**, 841-864.